

Studies of Cu/Ru(0001) and Cu/O/Ru(0001) Surfaces by LEIS, AES and LEED

*Y. G. Shen, J. Yao, D. J. O'Connor, K. Wandelt^A
and R. J. MacDonald*

Department of Physics, University of Newcastle, NSW 2308, Australia.

^A Permanent address: Institut für Physikalische und Theoretische Chemie der Universität Bonn, Wegelerstrasse 12, D-5300 Bonn 1, Germany.

Abstract

Studies of Cu/Ru(0001) and Cu/O/Ru(0001) surfaces were made by applying low energy Li⁺ and He⁺ ion scattering with a combination of Auger electron spectroscopy, low energy electron diffraction and computer simulation. It was found that Cu grew on Ru(0001) layer-by-layer for the first two layers. Using Li⁺ ions, the results obtained by analysing the incident angle dependence associated with shadowing of Ru by Cu confirmed that the first layer Cu was in a normal registry position, i.e. there was a continuation of the hexagonal close-packed stacking sequence. The second layer Cu was determined to be in registry along the long azimuth (one of three possible domains) by analysing the shadowing features for the second layer Cu focusing onto the first layer Cu atoms. The Cu/O/Ru(0001) surface was also studied by He⁺ ion scattering. During deposition of Cu, the great majority of oxygen (about 70%) originally on the clean Ru(0001) surface was found to float out onto the top of the growing Cu overlayers. This displacement process could be observed up to Cu coverages of 10 ML, which appeared to be independent of the deposition rate, the O precoverage and the substrate temperature. The floating O atoms in the top layer have been determined to be a disordered overlayer by measuring the azimuthal scan dependence at grazing incidence.

1. Introduction

The growth of thin films on metal substrates is a rapidly expanding field due to the fundamental importance of these systems in both heterogeneous catalysis and materials science. A thermodynamical criterion based upon the surface energies of the substrate (γ_s) and film overlayers (γ_f) and upon the interfacial energy (γ_{int}) has been traditionally established for predicting the growth mode (Bauer and ver der Merwe 1986). If the system minimises the surface free energy, then for $\Delta\gamma = \gamma_f + \gamma_{int} - \gamma_s < 0$ layer-by-layer (Frank-van der Merwe) growth is expected, while for $\Delta\gamma \geq 0$, three-dimensional (3D) (Volmer-Weber) growth is expected. It has been argued that in highly strained systems with $\Delta\gamma < 0$, the Stranski-Krastanov growth mode should also be predicted (with completion of the first layer followed by 3D growth in subsequent layers).

The growth of Cu on the hexagonal close-packed (hcp) Ru(0001) surface has been regarded as a prototypical bimetallic system for surface studies. Cu does not form an alloy with the Ru substrate. Many studies have been carried out by surface averaging techniques, such as Auger electron spectroscopy (AES),

low energy electron diffraction (LEED), thermal desorption spectroscopy (TDS) and work function measurements, concentrating mainly on the growth mode and the symmetry of the thin films (see e.g. Park *et al.* 1987; Houston *et al.* 1986, and references cited therein). However, little information about the atomic arrangement of the Cu films is given and so surface structures are often inferred from the coverage dependence of the work function change and LEED patterns. In addition, complications caused by the simultaneous presence of the surface domains of Ru(0001) are normally ignored. Recent scanning tunnelling microscopy (STM) measurements by Pötschke and Behm (1991) revealed the existence of two surface domains, showing pseudomorphic growth of the first Cu layer and a unidirectionally contracted second layer along the [100] azimuth. Very recently, LEED-IV analysis by Feibelman *et al.* (1994) also confirmed that the first layer Cu was in a normal registry position, but the surface domain effects were not identified. The effects of adding Cu by vapour deposition to an O-precovered Ru(0001) surface have also been investigated recently by Wandelt (one of the present authors) and his group using AES, TDS and work function measurements (Kalki *et al.* 1993; Wolter *et al.* 1993). The results indicated that there exists a continuous displacement of the oxygen to the surface during Cu deposition for a wide range of experimental conditions.

In the present study, the Cu/Ru(0001) and Cu/O/Ru(0001) surfaces have been studied by low energy ion scattering (LEIS) with a combination of AES, LEED and computer simulation. LEIS is well established as a probe for both surface composition and surface structure. Interest in LEIS as a structure technique has grown rapidly over the last ten years. Work on alkali ion beams, time-of-flight (TOF) scattering techniques, computer simulations and numerous structural determinations have established LEIS as a modern surface analysis technique (see e.g. reviews by Niehus *et al.* 1993; Rabalais 1989). The usual method for LEIS data analysis involves the concept of shadowing or blocking of substrate atoms to explain changes in reflected ion yield. The shadowing positions as a function of incident and azimuthal angles established the orientation between the atoms on the clean surface or between adsorbate and target atoms. By measuring the scattered or recoiled ion yield at specific scattering and recoiling angles as a function of incident angle α and azimuthal angle Φ to the surface, one can observe structures that can be interpreted in terms of the interatomic spacings based on the form of the scattering potential.

The purpose of this paper is twofold: first, to determine the structure of the Cu/Ru(0001) surface by low energy Li^+ ion scattering; second, to study the effects of the growth of Cu on an oxygen-precovered Ru(0001) surface at various experimental conditions with He^+ ions. An important point in these studies has to be emphasised here. The measurements on the Cu/O/Ru(0001) system were carried out with He^+ ions for two reasons. He^+ ions have an extremely high rate of neutralisation during scattering events, ensuring that the detected signal mainly comes from the outermost layer; for Li^+ scattering, O single scattering peaks are superimposed on a large background signal at lower kinetic energies owing to multiple, inelastic scattering of the Li^+ ions from the subsurface. Such a background can totally obscure LEIS O peaks. However, care has to be taken to include the possible angular-dependent neutralisation of the He^+ ions in the interpretation of the experimental results.

2. Experimental

(2a) Instrument

The angle resolved ion scattering system has been described previously (Shen *et al.* 1992a, 1994). The base pressure in the UHV chamber was 1×10^{-10} mbar (1 mbar \equiv 100 Pa). The chamber was equipped with a three-grid LEED system. The 1000 eV Li^+ or He^+ ions were well focused, mass separated and finally collimated. The ion scattering was analysed by a hemispherical electrostatic analyser ($\Delta E/E = 0.02$) with multichannel detection (MCD). The use of MCD allows data collection with small ion doses, typically at a beam current density of $\sim 2 \times 10^{-8}$ A cm^{-2} for He^+ ions and $\sim 3 \times 10^{-9}$ A cm^{-2} for Li^+ ions used in this study. No significant effect of ion induced damage and desorption was observed during the measurement. As a measure of the peak (Cu, Ru and O) intensities, the areas under the peaks were determined by using linear subtraction of the background. The detailed AES analysis was performed on the scanning Auger spectrometer in a separate UHV chamber.

(2b) Sample Preparation

The sample used in this study was 99.999% pure Ru single crystal aligned to within 0.5° of a (0001) surface using the Laue X-ray diffraction technique. The sample had been used and extensively cleaned in previous examinations by Kalki *et al.* (1992). The Ru(0001) sample was cleaned by using a standard procedure: by Ar^+ ion sputtering and many heating/cooling cycles between 600 and 1500 K in 2×10^{-7} mbar O_2 . Final cleaning was achieved by heating to 1550 K. Surface cleanliness was tested by either 1 keV He^+ ion scattering or AES measurements, which showed that O, S and C were absent.

High purity Cu was evaporated onto the Ru surface from a resistively heated W basket. The evaporation rate was typically 1 ML in four minutes. With the source well outgassed prior to Cu evaporation, the pressure increase during evaporation was 4×10^{-10} mbar or less. Oxygen exposure measurements were carried out by back-filling the chamber with 99.999% pure O_2 through a leak valve at a pressure of 5×10^{-8} mbar. All exposures reported here were based on uncorrected ion gauge readings.

(2c) Potential Calibration

The Li^+ ions were mainly used for structural determination because Li^+ has a small neutralisation probability, which makes it possible to get information not only from the first layer but also from the second or even third layers. To do so it is first necessary to determine the scattering potential for the interaction of projectiles and surface atoms. It is well known that the Thomas-Fermi-Molière (TFM) potential is approximated for describing the LEIS energy regime and is expressed by the formula

$$V(r) = \frac{Z_1 Z_2 e^2}{r} \Phi(r/a), \quad (1)$$

where

$$\Phi(x) = 0.35 \exp(-0.3x) + 0.55 \exp(-1.2x) + 0.10 \exp(-6x), \quad (2)$$

$$a = ca_F = ca_B 0.88534 (Z_1^{\frac{1}{2}} + Z_2^{\frac{1}{2}})^{-\frac{2}{3}}, \quad (3)$$

and where $Z_1 e$ and $Z_2 e$ are the number charges of projectile and target atoms respectively, a_F is the Firsov (1959) screening length, c is an adjustable parameter to improve agreement between calculation and experiment and to compensate for the fact that the TFM potential decays too slowly with increasing distance r , compared to the potential derived from Hartree–Fock calculations (O'Connor and Biersack 1986). The value of c is determined from measurement of the critical angle α_c as a function of scattering angle θ along a given azimuth for standard single crystals, and then compared with the calculated critical angle using the TFM potential with a fitted value of c (Shen *et al.* 1995).

(2d) Cu Coverage Calibration

Cu films on Ru(0001) deposited at room temperature with thicknesses ranging from 0.2 to 10 ML were studied. However, our main interest was concentrated on the low coverage regime ($\lesssim 2$ ML). The coverage was calibrated by AES, LEED and LEIS measurements.

The growth of Cu on Ru(0001) measured by AES is shown in Fig. 1*a*, where the AES peak-to-peak ratio $I = I_{\text{Cu}(920)}/I_{\text{Ru}(273)}$ between the intensity of the Cu AES line at 920 eV and the intensity of the Ru AES line at 273 eV is plotted as a function of Cu coverage. The Cu coverage is determined from the formula

$$I = I_\infty \frac{1 - e^{-d/\lambda_{920}}}{e^{-d/\lambda_{273}}}, \quad (4)$$

where $I_\infty = I_{\text{Cu}(920)}^\infty/I_{\text{Ru}(273)}^\infty$; I^∞ denotes the intensity of the AES line from a very thick sample of Cu at 920 eV and Ru at 273 eV, the λ are the inelastic mean free paths of electrons with 920 (273) eV energy travelling in Ru and d is the Cu film thickness (taken to be 2.56 Å) assumed to be uniform over the substrate surface. A layer-by-layer growth up to 2 ML obtained in Fig. 1*a* is also supported by the curve, which was calculated on the basis of the Gallon (1969) model assuming layer-by-layer growth.

Similar to the AES uptake curve, the Cu/(Cu+Ru) LEIS top layer intensity ratio obtained with He⁺ ions in Fig. 1*b* increases almost linearly with Cu coverage up to 1 ML where a distinct breakpoint in the slope is observed. On further increasing the Cu coverage up to 2 ML, the residual Ru signal remains just a few percent. This residual Ru signal is probably due to scattering from surface defects and/or domain edges. Fig. 1*c* shows that the Li⁺ single scattering intensity from Cu increases almost linearly with Cu coverage up to about 1 ML, which is in agreement with the He⁺ results. On further increasing the Cu coverage, the Cu signal increases due to the second layer Cu focusing onto the first layer Cu under this special scattering geometry. The almost linear increasing after 1 ML Cu coverage up to about 2 ML indicates layer-by-layer growth at least up to 2 ML.

Our LEED observation also supports the layer-by-layer growth of Cu up to 2 ML. Neither the additional LEED spots nor the significant increase of the background could be observed. During deposition, a six-fold symmetry of the hcp structure remained unchanged, indicating pseudomorphic growth up to 2 ML. At higher coverages the LEED pattern showed a three-fold symmetry, i.e. a Cu(111)-like structure. The good agreement in the Cu coverage obtained from the AES data, the model prediction, the LEED observation and the LEIS results

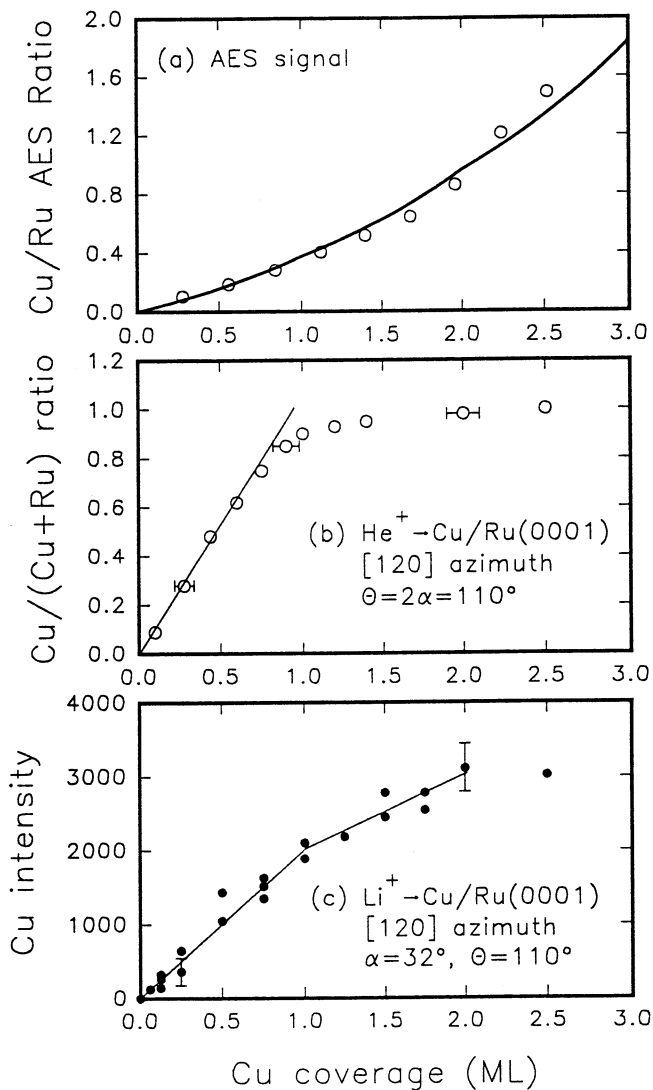


Fig. 1. (a) Cu(920 eV)/Ru(273 eV) peak-to-peak ratio as a function of the Cu coverage deposited at 300 K. The curve is the predicted behaviour based on layer-by-layer growth. (b) Normalised Cu/(Cu+Ru) intensity ratio of He⁺ ions and (c) intensity of the Li⁺-Cu single scattering peaks from the Cu covered Ru(0001) surfaces shown as a function of the Cu coverage. The lines are intended to guide the eye and representative error bars are indicated.

lends confidence to this determination. We estimate that the experimental error of the Cu coverage should be accurate to about $\pm 15\%$ but less than ± 0.20 ML.

The effect of annealing up to 900 K on the overlayer with coverage of ≤ 2 ML was negligible. No changes were observable in the ion scattering spectrum. Our AES data also confirmed that the Cu coverage did not change since the Cu AES signal did not decrease as a result of annealing.

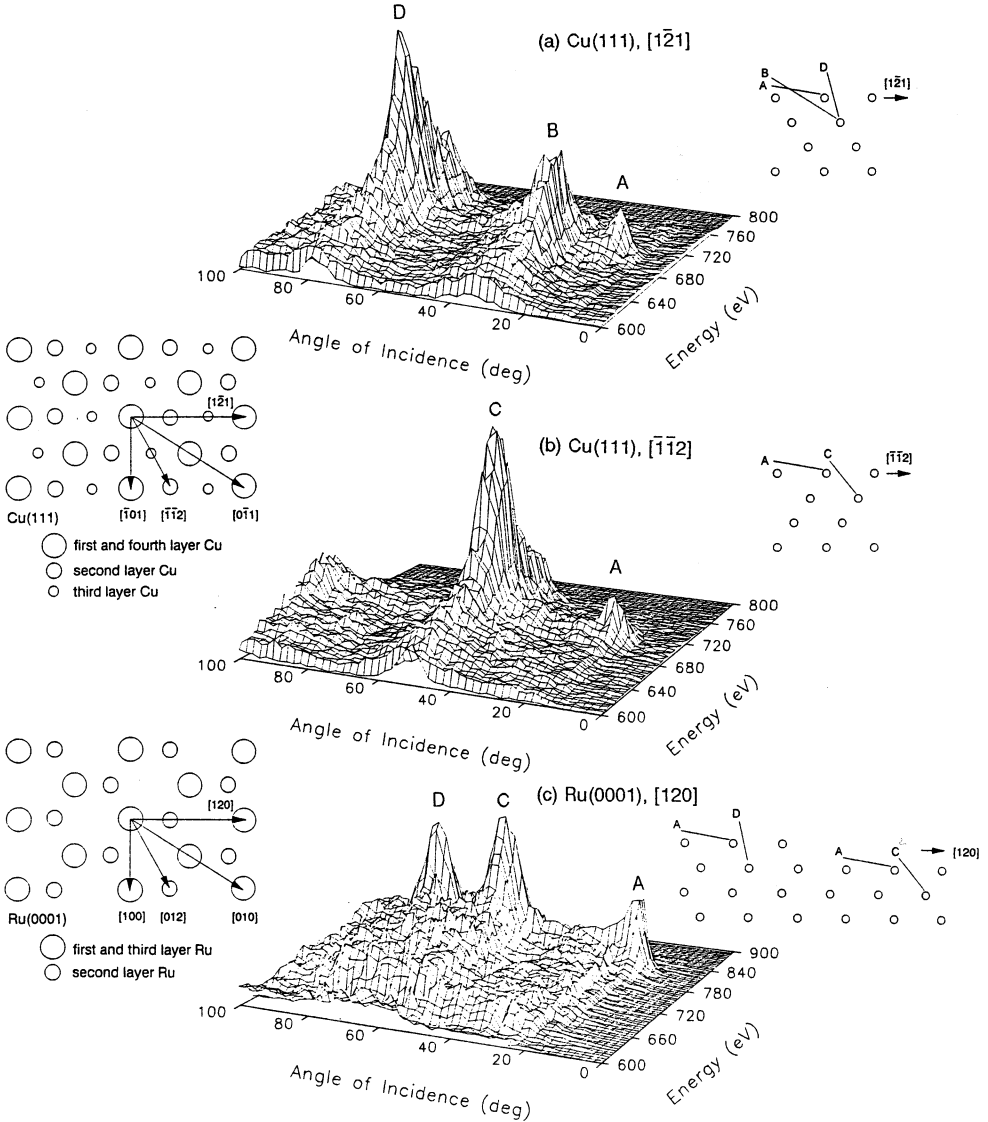


Fig. 2. Experimental LEIS energy and angle dispersive backscattered intensity distribution obtained from Cu(111) along (a) $[1\bar{2}1]$, (b) $[\bar{1}\bar{1}2]$, and from Ru(0001) along (c) $[120]$ with 1 keV Li^+ ions at a scattering angle of $\theta = 130^\circ$. Insets show the top views of Cu(111) and Ru(0001) as well as the scattering situations along three different azimuths. Note that a side view along the $[120]$ azimuth in Ru(0001) shows two domains.

3. Results and Discussion

(3a) Reference Systems: Ru(0001) and Cu(111)

Figs 2a–2c show energy and angle dispersive LEIS distributions for 1 keV Li^+ ions backscattered along the $[1\bar{2}1]$ and $[\bar{1}\bar{1}2]$ azimuths (separated by a rotation of 60°) in Cu(111) and the $[120]$ azimuth in Ru(0001) at a scattering angle of $\theta = 130^\circ$. These azimuthal orientations correspond to the long azimuthal

directions where the nearest distances are ~ 4.43 Å in Cu(111) and ~ 4.69 Å in Ru(0001) respectively. For each scan the ion intensity at small α values is low because each surface atom lies in the shadow cone cast by its preceding neighbour. By increasing α , the atoms of the first layer move out of the shadow cone at a critical angle α_c . As α increases further, scattering from the deeper layers may contribute to the scattered Cu or Ru signals. The critical angles for Cu and Ru scans in Figs 2a–2c reflect directly the position of atoms in the first, second and possible third layers. According to the computer simulation, the experimentally determined critical angle α_c corresponding to 80% of maximum intensity was used to define the position of the α_c (Shen *et al.* 1992b).

The most important feature in Fig. 2 is that there are three shadowing edges ($\alpha_c \approx 14^\circ$, 29° and 73°) in $[\bar{1}\bar{2}1]$ (Fig. 2a) and two critical angles ($\alpha_c \approx 14^\circ$ and 53°) in $[\bar{1}\bar{1}2]$ (Fig. 2b) for Cu(111), while there are three critical angles ($\alpha_c \approx 15^\circ$, 53° and 74°) in $[120]$ (Fig. 2c) for Ru(0001). These features are consistent with the structures and expected differences between hcp(0001) and fcc(111) surfaces, i.e. the presence of monatomic steps on the Ru(0001) surface has the consequence that both terminations are present at the same time. This is in good agreement with recent STM measurement (Pötschke and Behm 1991), which showed that the clean and well-annealed Ru(0001) surface formed extremely large, monatomic flat terraces, which often extend over 1000 Å or more and kink density was very low.

(3b) Structure of the Cu/Ru(0001) Surface

Fig. 3 shows the Ru incident angle α scans along the $[120]$ azimuth at $\theta = 130^\circ$, collected as a function of Cu coverage. In the presence of deposited Cu, the first shadowing peak where scattering occurs from only the first layer Ru atoms is attenuated. With increasing Cu coverage, the new shadowing peak appearing at around $\alpha = 29^\circ$ is observed. This is attributed to the first layer Cu focusing onto the first layer Ru because the Cu shadow cone is slightly smaller, allowing Li^+ ions at this incident angle to penetrate into the first Cu layer to scatter from the first layer Ru atoms. At a coverage of 1 ML the first shadowing peak is eliminated, while the new shadowing peak becomes pronounced. This is entirely consistent with pseudomorphic growth of the first Cu layer. The effect of Cu deposition is also to cause the decrease of shadowing peaks at higher incident angles. However, the shape of the two Ru shadowing edges at higher incident angles resulting from second and third layer scattering remains almost unchanged for coverages up to 2 ML. The fact that no extra shadowing features appear is in good agreement with LEED observations, confirming that the second layer Cu atoms are in normal registry positions, at least along this long azimuthal direction. The presence of the second Cu layer results in the disappearance of the Ru shadowing peak at around $\alpha = 29^\circ$. This is due to shadowing effects as expected.

To determine the Cu–Ru interlayer spacing precisely, the scattering potentials for the interaction of Li^+ –Cu and Li^+ –Ru have to be known. In this study, information about scattering potentials was obtained from measurement of the critical angles α_c as a function of scattering angle θ along one given azimuth for clean Cu(111) and Ru(0001), and then by fitting them to the critical angles calculated from the TFM potential with an adjustable parameter c . Based on the

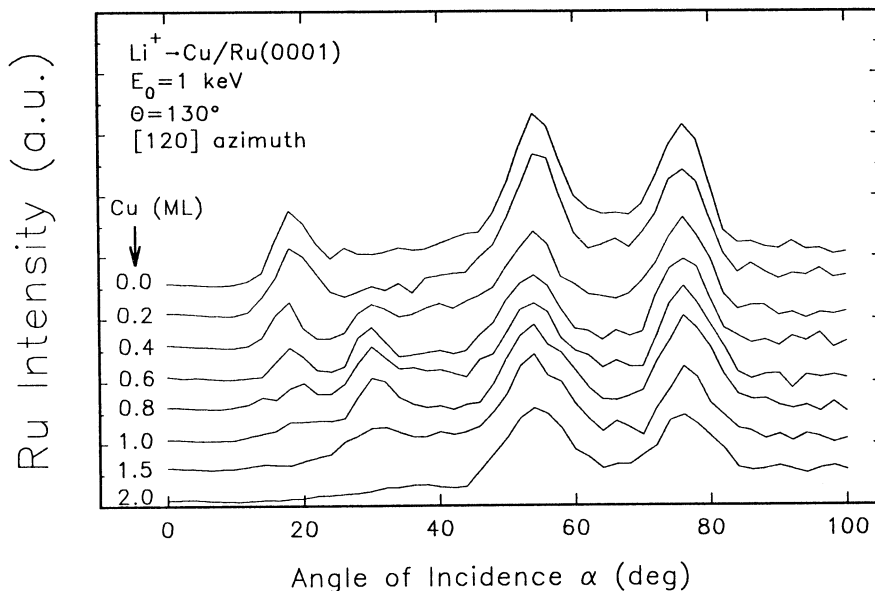


Fig. 3. Intensities of 1 keV Li^+ ions scattered from the Ru atoms as a function of incident angle α are shown for various coverages of deposited Cu in the [120] azimuth at $\theta = 130^\circ$.

known interatomic spacing along the long azimuth, we are able to determine the Li^+ -Cu and Li^+ -Ru scattering potentials. The theoretical critical angles were calculated using a chain model simulation. The values of $c_{\text{Cu}} = 0.80 \pm 0.04$ and $c_{\text{Ru}} = 0.85 \pm 0.05$ were obtained. This determination of the scattering potential using standard samples is not only an effective way to decide the c parameter, but also a self-calibration procedure. (For details of this determination procedure as well as the calculation method see Overbury *et al.* 1990; Shen *et al.* 1992*c*.)

Detailed experimental measurements have been carried out along the [120] azimuth at 1 ML coverage. The critical angles α_c for first layer Cu shadowing of first layer Ru were measured and compared to the calculated critical angles at three different scattering angles (90° , 110° and 130°). Since both clean and 1 ML Cu/Ru(0001) surfaces exhibited sharp 1×1 LEED patterns and no indications were found that either surface possessed a deviation from the hcp stacking sequence, it was only necessary to vary the interlayer spacing when calculating α_c . Fig. 4 shows plots of α_c as a function of the interlayer spacing, $D_{11}(\text{Cu-Ru})$. The mean value $D_{11}(\text{Cu-Ru}) = 2.10 \pm 0.05 \text{ \AA}$ obtained indicates that the Cu-Ru vertical distance has the Ru bulk interlayer spacing within the experimental uncertainty. The error in the Cu-Ru interlayer spacing was based on four or five different measurements.

The accuracy of the Cu-Ru interlayer spacing of the D_{11} depends on the accuracy of the critical angles measured and the accuracy of the critical values calculated by the simulation with the scattering potential. In evaluating the accuracy of this determination it is important to consider the effects of broadened shadowing edges due to thermal vibrations, multiple scattering, instrumental effects and the imperfections in the surface structure. By trying different measurements,

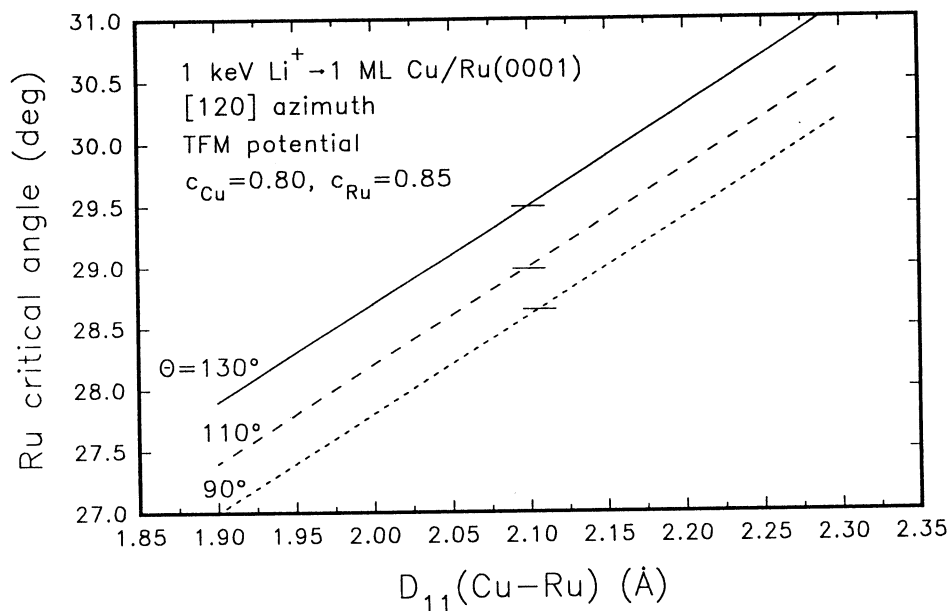


Fig. 4. Calculated Ru critical angles α_c at 1 ML coverage in the [120] azimuth for scattering from the first layer Ru atoms are shown as a function of the interlayer spacing $D_{11}(\text{Cu-Ru})$. The calculation was performed at three different scattering angles using the TFM potential with values of $c_{\text{Cu}} = 0.80$ and $c_{\text{Ru}} = 0.85$. The measured critical angles are indicated by the short horizontal lines (for detail see text).

it is estimated that an error of $\pm 0.5^\circ$ can be introduced. Another consideration in the accuracy of the critical angles α_c measured is due to the uncertainty in the scattering potential. In this study, the TFM potential was calibrated directly along the known interatomic spacings on Cu(111) and Ru(0001). Our calculation indicates that the determination of the critical angle α_c for first layer Cu shadowing of first layer Ru is very sensitive to the value of the parameter c_{Cu} (shadowing atom) rather than c_{Ru} (scattered atom). For example, we calculated that variation of the value of c_{Ru} by ± 0.1 only changes the predicted α_c by $\pm 0.1^\circ$, while variation of c_{Cu} by this amount changes α_c by 0.8° . An uncertainty of $\delta c_{\text{Cu}} = \pm 0.04$ obtained in this study, which causes an error of $\delta \alpha_c = \pm 0.4^\circ$ at most, will give a sufficient accuracy for our purpose. If we also consider the uncertainty of the α value to be $\sim 0.5^\circ$, the total uncertainty of the critical value α_c is about $\delta \alpha_c \sim \pm 1.0^\circ$. It can be concluded that the Cu-Ru interlayer spacing has the Ru bulk interlayer spacing within 0.05 \AA .

Further information for the structure at 1 and 2 ML Cu coverages is provided by the α scan of the Li^+ -Cu single scattering peak along the [012] and [120] azimuths shown in Fig. 5a. The general feature for Cu deposition along both azimuths is the same, resulting in the sharp first Cu shadowing edge at around $\alpha_c = 14^\circ$ at 1 ML. This is due to first layer Cu shadowing of first layer Cu. The second shadowing edge at around $\alpha = 28^\circ$ becomes pronounced at coverage of 2 ML. The most important feature for these two scans is that the Cu α scan at 2 ML coverage shows almost similar shadowing features along both long azimuths. The reason for this is the presence of two domains in the surface, leading to

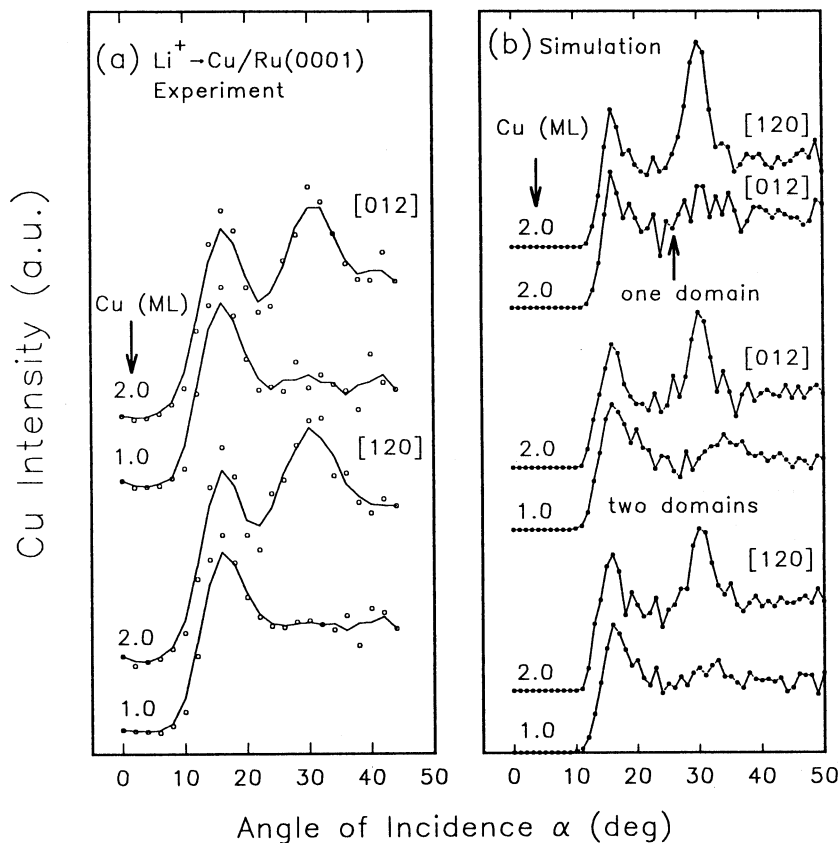


Fig. 5. Intensities of 1 keV Li^+ ions scattered from the Cu atoms as a function of incident angle α are shown for 1 and 2 ML coverages along the [012] and [120] azimuths at $\theta = 130^\circ$: (a) experimental α scans and (b) simulated α scans with and without two domains.

an averaging of the α scan. To determine the configuration of the first two Cu layers precisely, 3-D SABRE (O'Connor 1979) simulations of the α scans have been performed. When simulating the α scans, the ABAB... stacking order of the hcp structure was assumed. Fig. 5b shows the simulated α scans along the [012] and [120] azimuths with and without two surface domains. For the absence of surface domains, the features of the simulation along the [120] azimuth are considerably different from that along the [012] azimuth for $\alpha \approx 26^\circ$ – 33° . This is due to the fact that along the [120] azimuth the Li^+ ions can penetrate into the second Cu layer to scatter from the first Cu layer at these incident angles, while along the [012] azimuth this is not possible due to shadowing effects. For the presence of two domains, the simulation reproduces the experimental α scans along both azimuths with the exception of the narrow and sharp shadowing features. Discrepancies are within the angular resolution used in both experiment and simulation. From Fig. 5b it can be concluded that the best agreement with the experimental α scans was achieved for a simulation with the presence of two domains. Simulations with different interatomic spacings in the range of $2.5 \sim 2.9 \text{ \AA}$ along the short azimuth [100] gave similar results (note that the interatomic spacing along [100] in Ru(0001) is 2.71 \AA).

We have to point out that the existence of the second Cu layer in the two different terrace levels makes it difficult to distinguish whether the second layer Cu has either the stacking order ABAB... of the hcp structure or ABCABC... of the fcc structure. Our LEED observation and the α scan from the Ru single scattering (Fig. 3) support the ABAB... stacking, at least along the long azimuthal direction (one of three possible domains). The ABAB... stacking is also favoured in the literature (Pötschke and Behm 1991), while along the short azimuth the second Cu layer is contracted by $\sim 5.5\%$. This contraction could not be evidenced from ion scattering results only because of some lack of sensitivity with respect to atomic movements parallel to the surface.

The structure of the Cu layers up to 6 ML has also been probed not only by measuring the incident angle scan but also azimuthal angle. The results from the α scan in Fig. 6a suggest that the structure of 6 ML Cu/Ru(0001) is similar to Cu(111) although some distortion was observed. At higher coverages Cu(111)-like films with several incompleting layers might explain this distortion. From the same shadowing critical values of both Cu(111) and 6 ML Cu/Ru(0001), we believe that for thicker Cu films, an effective isotropic contraction must be achieved so that the lattice can finally reach the Cu(111) geometry. The fact that the large shadowing dips centred at $\Phi = 15^\circ$, 45° and 75° corresponding

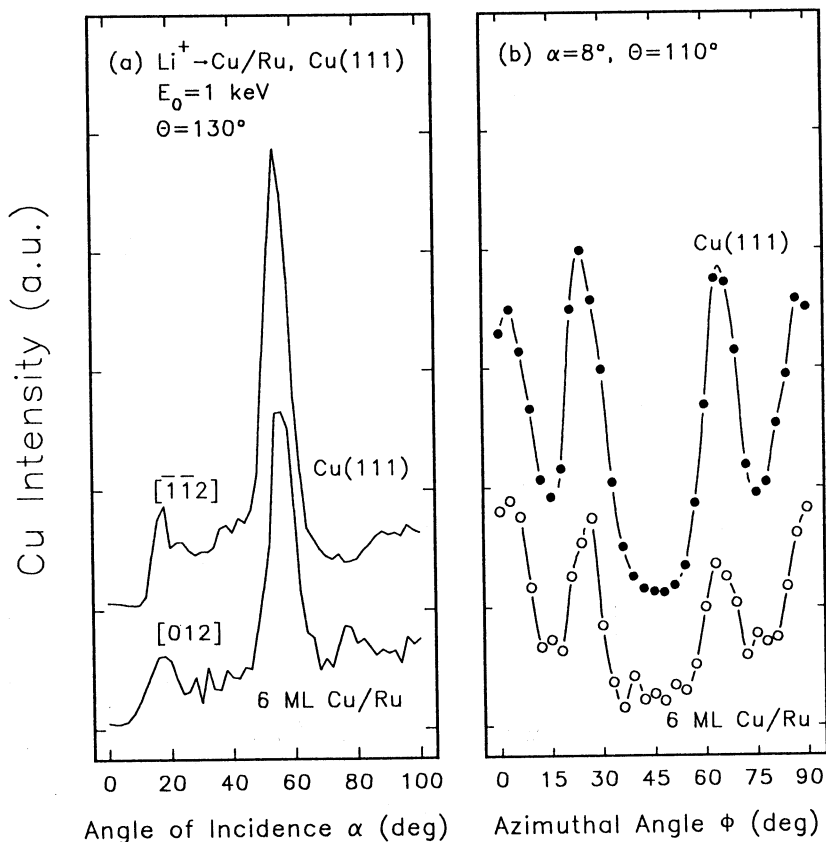


Fig. 6. Comparison between 6 ML Cu-covered Ru(0001) surface and a clean Cu(111) surface using 1 keV Li^+ ions: (a) incident angle scans and (b) azimuthal angle scans.

to rows of the Cu atoms aligned in these directions do not shift in azimuth with 6 ML Cu/Ru(0001) demonstrates directly that the film orientation relative to the substrate is not altered.

(3c) Cu Deposition on an O-precovered Ru(0001) Surface

Adsorption of O on Ru(0001) forms two ordered structures: the $p(2\times 2)O$ islands at coverage of 0.25 ML and $p(2\times 1)O$ phase at 0.5 ML (Madey *et al.* 1975; Pfnür *et al.* 1989). In the present article the measurement of absolute O coverage on Ru(0001) was based on the sharpest $p(2\times 2)O$ and $p(2\times 1)O$ LEED patterns with known structures. We define the adsorption of 4 L and 15 L in the temperature range from 300 to 523 K corresponding to the O coverage of 0.25 and 0.5 ML respectively.

Fig. 7 shows example plots of the LEIS He^+ spectra collected as a function of Cu coverage from an 0.5 ML O-precovered Ru(0001) surface, deposited at 300 K. Additional reference spectra from clean and 0.5 ML O/Ru(0001) surfaces are also shown. In this experiment, special care was taken to minimise sputtering-induced

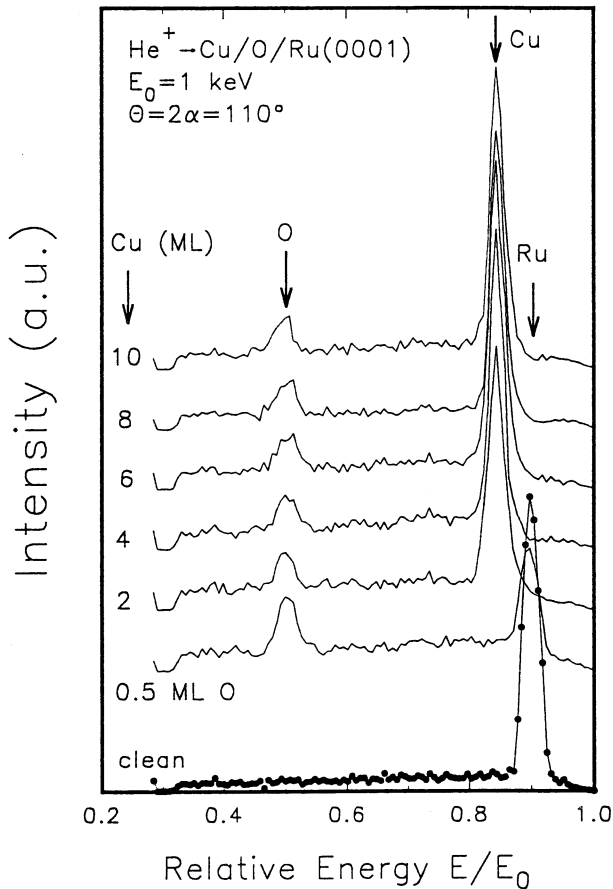


Fig. 7. Energy spectra of 1 keV He^+ ions scattered from clean, 0.5 ML O-covered and Cu/O/Ru(0001) surfaces at various coverages of Cu at 300 K.

damage, roughening and selective removing of oxygen by the ion beam. Sputtering of the O was experimentally measured to be less than 0.02 ML for the time required to collect each spectrum (10 s). As Cu is deposited, the Cu signal increases, and the Ru signal decreases. The Ru signal is almost undetectable at a Cu coverage >1 ML. The most interesting feature for this observation is that the great majority of oxygen (about 70%) originally on the clean Ru(0001) surface is still present following large amounts of Cu deposition on the top of the O layer. This displacement process could be observed up to Cu coverages of 10 ML. Further deposition after 10 ML coverage was not attempted owing to the effects of residual gas adsorption from the ambient. This observation supports the result obtained from the AES measurements (see Fig. 1 in Kalki *et al.* 1993), although Kalki *et al.* found a constant amount of 85% floating O on the top of the deposited Cu surface. A possible explanation for the discrepancy between the AES data and our results is the different surface sensitivity between AES and LEIS.

To give an idea of the effect of the floating O at different O precoverages and substrate temperatures, a systematic study of thin Cu films on an O-precovered Ru(0001) surface was performed. The LEIS spectra were recorded after successive Cu deposition. The normalised O intensity value, i.e. the ratio of the O signal in the Cu/O/Ru surface to that of the original value in the O/Ru surface, is then a direct measure of the number of the floating O atoms. These results are shown in Fig. 8. The general behaviour in all cases is quite similar. During the

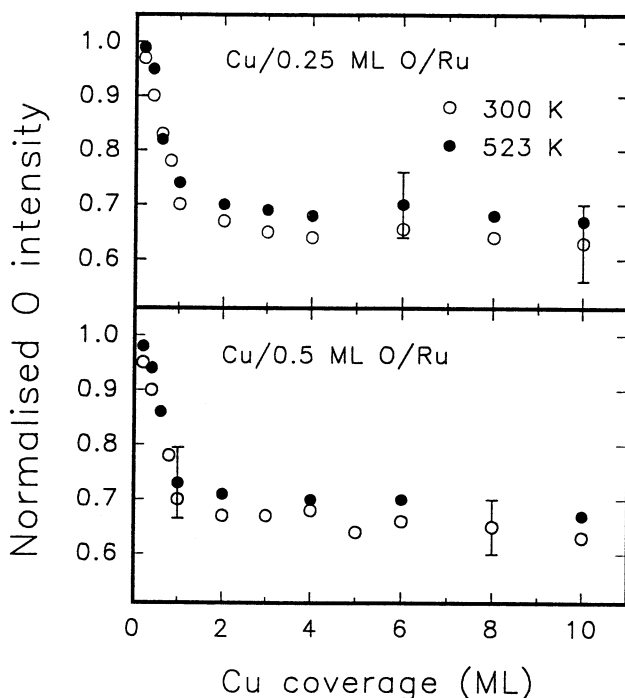


Fig. 8. Normalised O intensity obtained after Cu evaporation onto 0.25 ML O/Ru(0001) and 0.5 ML O/Ru(0001) surfaces at two different substrate temperatures as a function of Cu coverage.

deposition of the first Cu ML (240 s), the O signal decreases by about 30% of its original value and then remains almost constant. This feature occurs for a wide range of experimental conditions. The behaviour of the floating O is found to be independent of the O precoverage (\leq saturation coverage of 0.5 ML), Cu deposition rate (whether a 10 ML Cu film was deposited dose-wisely or once) and substrate temperature in the range 300 to 523 K.

To further understand the influence of the floating O on the growing Cu thin film and to determine ordering of the displaced O layer, an azimuthal scan was performed. It is known that the symmetry and ordering of the top layer atoms can be effectively obtained from the Φ scan. Fig. 9 shows the results of the Φ scan for 6 ML Cu/0.5 ML O/Ru(0001) at $\alpha = 8^\circ$ and $\theta = 60^\circ$. For comparison, the Φ scan for the 6 ML Cu/Ru(0001) surface under the same experimental conditions is used as a reference, also shown in Fig. 9. From these scans the following three statements can be made: (i) The Cu signal in the Cu/Ru(0001) surface exhibits three pronounced minima located at azimuthal angles of 15° , 45° and 75° , corresponding to the main azimuthal orientations in the Cu(111)-like surface

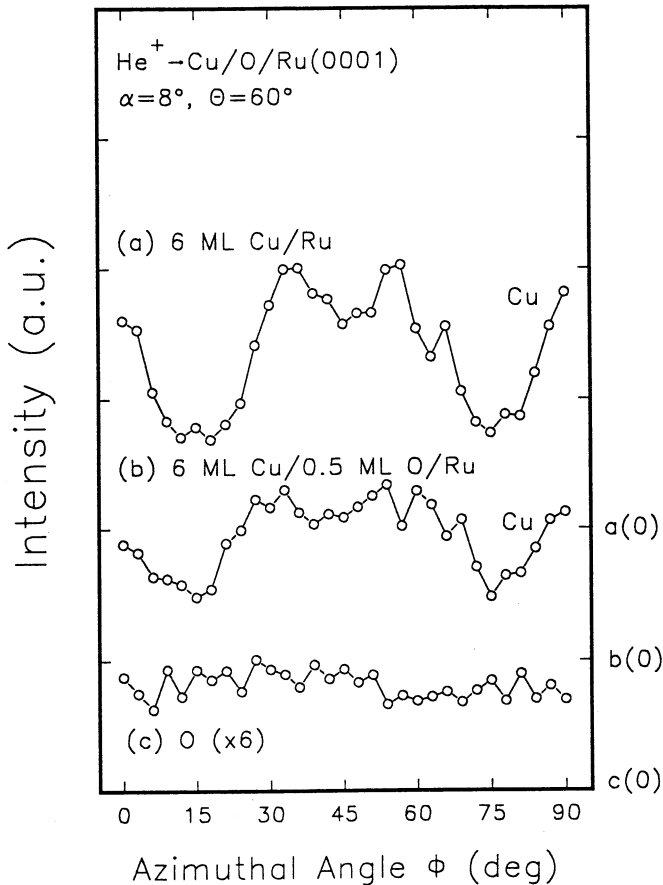


Fig. 9. Azimuthal scan dependence of 1 keV He^+ ions shows (a) the Cu scan from 6 ML Cu/Ru(0001), (b) the Cu scan and (c) the O scan from 6 ML Cu/0.5 ML O/Ru(0001) at 300 K.

(Niehus 1983). (ii) In the presence of the floating O atoms, the Cu scan for the Cu/O/Ru(0001) surface shows less pronounced dips along the main azimuthal directions compared to those for the Cu/Ru surface, indicating the occurrence of a less ordered overlayer. (iii) The floating O intensity is independent of the azimuthal angle, which suggests that the displaced O atoms may be randomly located in or above the top Cu layer. No shadowing or blocking effects in the O layer are found. We conclude that the displaced O may not form an ordered layer. These observations have been supported by LEED data. Upon deposition of Cu on 0.5 ML O/Ru(0001), the $p(2 \times 1)O$ pattern (three domains) grew increasingly diffuse until it disappeared at a Cu coverage of $\gtrsim 0.3$ ML. We suggest that at this stage the surface has either lost order within the O islands or consisted of ordered domains too small to provide a LEED pattern. With increasing Cu coverage on O/Ru, the LEED pattern shows the 1×1 structure with an increase in the background. No additional spots were observed after facile migration of O atoms from the Ru to the Cu layers has occurred. A similar LEED observation holds for Cu deposition on 0.25 ML O/Ru(0001) surface. The fact that a loss of the $p(2 \times 1)O$ LEED pattern [also the $p(2 \times 2)O$ pattern] appeared in early stages of Cu deposition and the background was high with increasing Cu coverage is entirely consistent with the results of the azimuthal scan shown above.

4. Discussion

The initial growth behaviour of metal thin films on metal substrates is determined by energetic and kinetic factors. From a thermodynamical point of view the system tends to form the energetically most favourable configuration, while kinetics determine the growth behaviour of the film. The values of surface free energy for Cu and Ru are 1.85 and 3.05 J m^{-2} (Mezey and Giber 1982) respectively. These values correctly predict layer-by-layer growth for Cu on Ru(0001). However, the difference in the lattice mismatch ($\sim 5.5\%$) between Cu and Ru is important for the structure and orientation of the film. Furthermore, the difference in adsorbate-substrate and adsorbate-adsorbate interactions plays a key role in the formation and stability of films beyond a monolayer. The strong tendency of the first Cu layer toward pseudomorphic growth evidenced by LEED and low energy Li^+ ion scattering reflects its relatively strong Cu-Ru interaction. The experimental observation that a pseudomorphic second Cu layer is formed along the long azimuth without rearrangement of the first Cu layer implies the strong substrate-substrate interaction of Cu.

Using ion scattering the Cu-Ru interlayer spacing was measured to be $2.10 \pm 0.05 \text{ \AA}$. The extent of this Cu-Ru surface spacing was determined directly from the α_c for the Ru single scattering. This determination of the $D_{11}(\text{Cu-Ru})$ is direct, and independent of the Ru first-second interlayer spacing and possible relaxation in the second or deeper layers. In the calculation of the critical angles, Li^+ -Cu and Li^+ -Ru scattering potentials were calibrated using standard Cu(111) and Ru(0001) samples. An advantage of ion scattering is, unlike electron and atom diffraction, that it provides mass-selective real-space information on the atomic arrangement at the surface without requiring sophisticated model calculations. From the results the second Cu layer is also in registry along the $[120]$ azimuth (one of three possible domains). However, it is difficult

in using ion scattering shadowing and blocking analysis only to determine whether the second Cu layer atoms are contracted slightly along the [100] azimuth.

In a previous study on the Au/O/Ru(0001) system, Bludau *et al.* (1990) have shown that Au grew in a layer-by-layer model on a clean Ru(0001) surface. However, it formed 3D islands even at very small coverages at an O-covered Ru surface. It is obvious that the presence of the surface O has influenced the Au growth behaviour. As a general rule the O pre-adsorption can reduce the surface free energy of a metal surface, thus leading to a change of the growth mechanism of the second metal. Recently, in a number of cases it was found that when a small amount of surface active species, a so-called 'surfactant' is preadsorbed on the substrate before growing the film, this surfactant lowers the surface free energy and permanently floats out onto the surface during the film growth. For the case of the Cu/O/Ru system, the role of the O seems to be to lower the surface free energy in such a way that a layer-by-layer growth of the Cu film is energetically favoured (Wolter *et al.* 1993). A recent TDS experiment by Kalki *et al.* (1993) showed the simultaneous desorption of O and Cu, indicating that the O-Ru interaction energy becomes comparable to the O-Cu interaction. Therefore, energetically the adsorbed O atoms no longer have a preference for Ru sites, leading the majority of O atoms originally located on the Ru substrate to migrate onto the growing Cu layer. The floating O layer reduces the overall energy of the film/substrate composite by lowering the surface free energy. This floating process could be detected by dynamical AES even for films as thick as 50 layers or for substrate temperatures as low as at 100 K (Kalki *et al.* 1993). The possibility of interdiffusion of O into the films is energetically unfavourable due to the small solid solubility of O in Cu (<0.001%) (Wolter *et al.* 1993) in the temperature range detected here.

A similar floating phenomenon has been seen in a few other systems, such as Cu/O/Cu(100) and Ni/O/Cu(100), where it was reported by Egelhoff and Steigerwald (1989) that for Cu deposition all the O floats out even at 100 K, while for Ni deposition only about 50% floats out at 100 K. However, the exact mechanism for this kind of float-out process is still not known. For example, the Cu/Ru and Au/Ru systems are very similar, but the floating O behaviour was not observed for the Au/O/Ru system. From a consideration of chemical interaction, we may get a reasonable explanation. It has been observed that Cu interacts chemically with O, forming CuO (Wolter *et al.* 1993) or Cu₂O (Jensen *et al.* 1991) on Cu(111), while such a chemical interaction between Au and O on Ru(0001) is not expected.

Clearly, for the floating process studied here involving a small portion of the O adatoms, AES data may not be sensitive enough to detect such subtle but important segregation processes. The main advantage for analysing the floating process by LEIS with He⁺ ions is that He⁺ ions are almost 100% neutralised for ions penetrating into the second or deeper atomic layers. Therefore, low energy He⁺ ion scattering has an extremely high sensitivity during scattering events, ensuring that the detected O signal mainly comes from the outermost layer. As no evidence has been found to warrant serious consideration of the possible angular-dependent neutralisation and the matrix effects, the effects of such processes have been ignored in the analysis.

5. Conclusions

The growth and structure of Cu on the Ru(0001) surface have been investigated using a combination of low energy alkali ion scattering, AES, LEED and computer simulation. It was found that Cu grew layer-by-layer for the first two layers. The Li⁺ ion scattering results indicate that the first layer Cu atoms are in normal registry positions. The Cu-Ru interlayer spacing was determined to be 2.10 ± 0.05 Å. These results are compatible with interpretations of very recent LEED-IV data (Feibelman *et al.* 1994). The second layer Cu atoms are also in registry along the long azimuth (one of three possible domains). However, along the short azimuth the second Cu layer may be contracted based on STM images (Pötschke and Behm 1991), though we cannot give evidence from ion scattering results only because of some lack of sensitivity with respect to atomic movements parallel to the surface. The structure of the Cu thin films up to 6 ML has also been probed by measuring the α and Φ scans. The result is consistent with an epitaxial Cu(111) structure by comparing with the results of Cu(111), although some distortion was observed.

Using He⁺ ion scattering it has been possible to obtain some interesting results on the growth of thin Cu films on an O-precovered Ru(0001) surface. Three conclusions are strongly supported by the results. Firstly, the great majority of oxygen (about 70%) originally on the clean Ru(0001) surface floats out onto the growing Cu layer following large amounts of Cu deposition on top of the O layer. This displacement process could be observed up to Cu coverages of 10 ML. Secondly, facile migration of O atoms from the Ru onto the Cu films seems independent of the O precoverage, the Cu evaporation rate and the substrate temperature. Thirdly, the displaced O from the Ru to the Cu film apparently shows no order related to the growing Cu films.

Acknowledgments

The authors are grateful to the Australian Research Council for financial support of this work. One of us (J. Yao) would like to thank the University's support through the provision of a scholarship. K. Wandelt also acknowledges the Deutsche Forschungsgemeinschaft for granting his research stay in the Department of Physics at the University of Newcastle.

References

- Bauer, E., and van der Merwe, J. H. (1986). *Phys. Rev. B* **33**, 3657.
- Bludau, H., Skottke, M., Pennemann, B., Mrozek, P., and Wandelt, K. (1990). *Vacuum* **41**, 1106.
- Egelhoff, Jr. W. F., and Steigerwald, D. A. (1989). *J. Vac. Sci. Technol. A* **7**, 2167.
- Feibelman, P. J., Houston, J. E., Davis, H. L., and O'Neill, D. G. (1994). *Surf. Sci.* **302**, 81.
- Firsov, O. B. (1959). *Sov. Phys. JETP* **36**, 1076.
- Gallon, T. E. (1969). *Surf. Sci.* **17**, 486.
- Houston, J. E., Peden, C. H. F., Blair, B. S., and Goodman, D. W. (1986). *Surf. Sci.* **167**, 427.
- Jensen, F., Besenbacher, F., Lægsgaard, E., and Steensgaard, I. (1991). *Surf. Sci. Lett.* **259**, L774.
- Kalki, K., Schick, M., Ceballos, G., and Wandelt, K. (1993). *Thin Solid Films* **228**, 36.
- Kalki, K., Wang, H., Lohmeier, M., Schick, M., Milun, M., and Wandelt, K. (1992). *Surf. Sci.* **269/270**, 310.
- Madey, T. E., Engelhardt, H. A., and Menzal, D. (1975). *Surf. Sci.* **48**, 304.
- Mezey, L. Z., and Giber, J. (1982). *Japan. J. Appl. Phys.* **21**, 1569.

- Niehus, H. (1983). *Surf. Sci.* **130**, 41.
- Niehus, H., Heiland, W., and Taglauer, E. (1993). *Surf. Sci. Rep.* **17**, 213.
- O'Connor, D. J. (1979). PhD thesis, Australian National University.
- O'Connor, D. J., and Biersack, J. P. (1986). *Nucl. Instrum. Meth. B* **15**, 14.
- Overbury, S. H., Mullins, D. R., and Wendelken, J. F. (1990). *Surf. Sci.* **236**, 122.
- Park, C., Bauer, E., and Poppa, H. (1987). *Surf. Sci.* **187**, 86.
- Pfnür, H., Held, G., Lindroos, M., and Menzel, D. (1989). *Surf. Sci.* **220**, 43.
- Pötschke, G. O., and Behm, B. J. (1991). *Phys. Rev. B* **44**, 1442.
- Rabalais, J. W. (1989). *Science* **250**, 521.
- Shen, Y. G., O'Connor, D. J., and MacDonald, R. J. (1992a). *Aust. J. Phys.* **44**, 12.
- Shen, Y. G., O'Connor, D. J., and MacDonald, R. J. (1992b). *Nucl. Instrum. Meth. B* **66**, 441.
- Shen, Y. G., O'Connor, D. J., and MacDonald, R. J. (1992c). *Surf. Interface Anal.* **18**, 729.
- Shen, Y. G., O'Connor, D. J., Wandelt, K., and MacDonald, R. J. (1994). 'Springer Proceedings in Physics' (Springer: Berlin), in press.
- Shen, Y. G., O'Connor, D. J., Wandelt, K., and MacDonald, R. J. (1995). *Surf. Sci.* **328**, 21.
- Wolter, H., Schmidt, M., and Wandelt, K. (1993). *Surf. Sci.* **298**, 173.

Manuscript received 8 December 1994, accepted 23 February 1995